

Efficiency droop behaviors of InGaN/GaN multiple-quantum-well light-emitting diodes with varying quantum well thickness

Y.-L. Li,^{a)} Y.-R. Huang, and Y.-H. Lai

Institute of Photonics and Optoelectronics, National Taiwan University, Taiwan 10617, Republic of China

(Received 13 September 2007; accepted 12 October 2007; published online 31 October 2007)

InGaN/GaN multiple-quantum-well (MQW) light-emitting diodes with varied InGaN quantum well thicknesses are fabricated and characterized. The investigation of luminous efficiency versus current density reveals a variety of efficiency droop behaviors. It is found that the efficiency droop can be drastically reduced by increasing the quantum well thickness of the MQW structures. On the other hand, relative internal quantum efficiency (IQE) measurements indicate that a thinner well results to higher IQEs owing to the greater spatial overlap of electron and hole distribution functions. © 2007 American Institute of Physics. [DOI: 10.1063/1.2805197]

InGaN/GaN based high-brightness light-emitting diodes (LEDs) have attracted much attention because of their applications in signage, back lighting, and general illumination. Many efforts have been made to improve material quality,^{1,2} light extraction efficiency,³ and metal-semiconductor Ohmic contacts.⁴ In addition, emission efficiencies of InGaN/GaN LEDs have been improved drastically during the last few years. As LED technology becomes more and more mature, it is highly desirable for LEDs to emit a high luminous flux at high current densities. However, for InGaN/GaN multiple-quantum-well (MQW) LEDs, a well-known fundamental problem needs to be overcome, namely, the efficiency “droop,” which is the reduction in efficiency as the current is increased.^{5,6} The strong efficiency droop is not observed for other material systems, such as AlGaInP–GaAs, and it is not very clear what mechanism causes the droop in InGaN/GaN material system.

In this letter, InGaN/GaN-based blue LEDs with various quantum well thicknesses are investigated. Electrical and optical characteristics of the LEDs are presented and discussed. The InGaN/GaN MQW LED samples used in this study are grown on a *c*-plane (0001) sapphire substrate with a Veeco metal-organic chemical vapor deposition system using a high speed rotating disk with a vertical gas-flow growth chamber. Trimethylgallium (TMGa), trimethylindium (TMIn), trimethylaluminum (TMAI), and ammonia (NH₃) are used as source materials of Ga, In, Al, and N, respectively. Bicyclopentadienyl magnesium (Cp₂Mg) and silane (SiH₄) are used as the *p*-type and *n*-type doping precursors, respectively. On top of the sapphire substrate, a 20 nm thick GaN nucleation layer is grown at low temperature followed by a thick (4 μm) *n*-type GaN buffer layer.

After buffer layer growth, a ten-period InGaN/GaN MQW active region on top of the buffer layer is grown. Triethylgallium (TEGa) is used as the Ga source material for the MQW growth. The growth rates for both barriers and wells are controlled at about 1.5 nm/min. Note that all barriers are doped with Si whereas the wells are left undoped. A thin (10 nm) Mg doped *p*-type AlGaInN is grown on top of MQW and followed by two sets of *p*-type AlGaIn/GaN (10 nm/2 nm) layers which serve as electron-blocking layer. Finally, a Mg doped *p*-type GaN cladding layer (120 nm) is

grown where the top region of the cladding layer is heavily Mg doped to facilitate Ohmic contact formation. For processing, LED chips (350 × 350 μm²) utilizing transparent conducting indium tin oxide layers are fabricated using a standard LED process.⁷ Ni/Au and Ti/Al/Ti/Au metallizations are deposited by e-beam evaporation to serve as *p*-type and *n*-type Ohmic contacts, respectively. The schematic structure of the processed LED samples is shown in Fig. 1.

This study has the purpose to understand the relationship between the efficiency droop and the thickness of the quantum wells. The barrier thickness of the MQWs is fixed at 12 nm while the thickness of the well is varied by changing the growth time. The growth times of each well in these samples are 1 min (1.5 nm), 0.8 min (1.2 nm), 0.6 min (0.9 nm), and 0.4 min (0.6 nm), respectively.

As-grown wafers are characterized by measuring photoluminescence as a function of temperature. The experiments are performed using a 10–300 K variable-temperature cryostat. The samples are optically pumped with a 50 mW He–Cd laser emitting at 325 nm. After chip fabrication, LEDs are characterized with a wafer prober. dc and pulsed currents are injected by a Keithley 2400 source meter. Electroluminescence (EL) spectrum and intensities are measured by a high-resolution spectrometer with an optical fiber collecting the light emitted from the top of the LED.

The temperature-varied photoluminescence (PL) measurement, shown in Fig. 2, gives the relative internal quantum efficiencies (IQEs) for these samples at room tem-

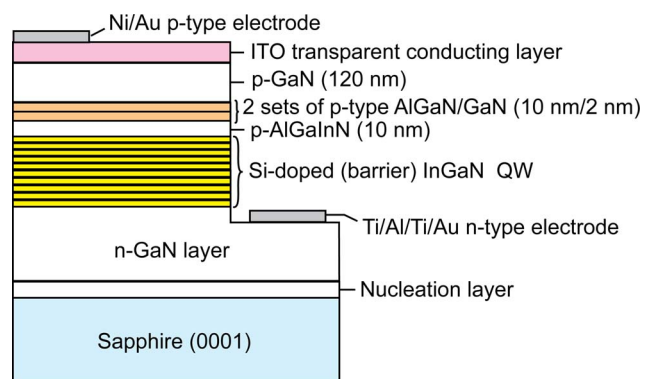


FIG. 1. (Color online) Schematic structure InGaN/GaN multiple-quantum-well LEDs with varied well thicknesses.

^{a)}Electronic mail: yunli@cc.ee.ntu.edu.tw

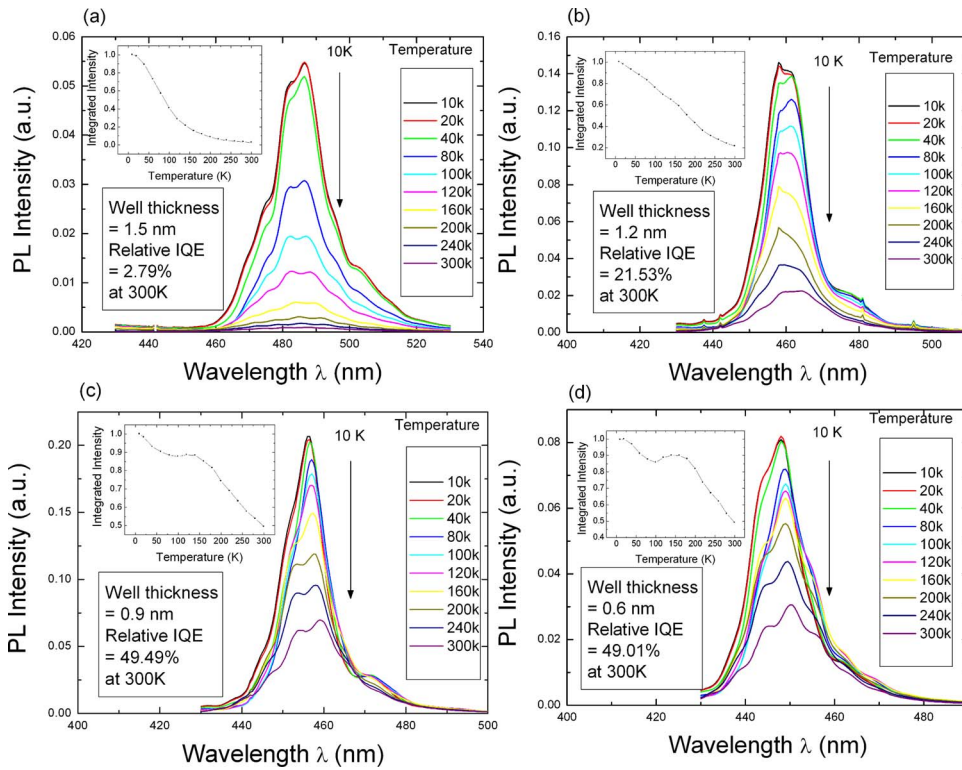


FIG. 2. (Color online) Temperature-varied (from 10 to 300 K) photoluminescence measurements for room-temperature IQE assessment of InGaN/GaN MQW LEDs with varied well thicknesses.

perature. It is known that the carrier recombination is dominated by nonradiative recombination at a room temperature in the InGaN/GaN system, whereas at low temperatures, it is dominated by radiative recombination. The relative IQE is estimated by comparing the low temperature (10 K) with the RT-PL (300 K) assuming that the PL internal quantum efficiency at low temperature (10 K) is equal to 1. The inspection of Fig. 2 reveals that the thicker the wells are, the lower the relative IQE at room temperatures. This is attributed to the larger electron-hole charge separation induced by internal field with thicker wells.^{8,9}

Room-temperature EL spectra under different pulsed injection currents are shown in Fig. 3. The pulsed currents have a 5% duty cycle and the pulsed injection duration is 3 ms. Figure 3 shows that the peak of the emission spectrum shifts toward shorter wavelengths (blueshift) with increasing injection currents. It is also shown in the figure that less blueshift is observed for MQWs with thinner wells. This can be explained by Coulomb screening of the piezoelectric-field-induced quantum confined Stark effect (QCSE), that is, the internal polarization field is compensated by injecting carriers. The blueshift phenomenon is due to the compensa-

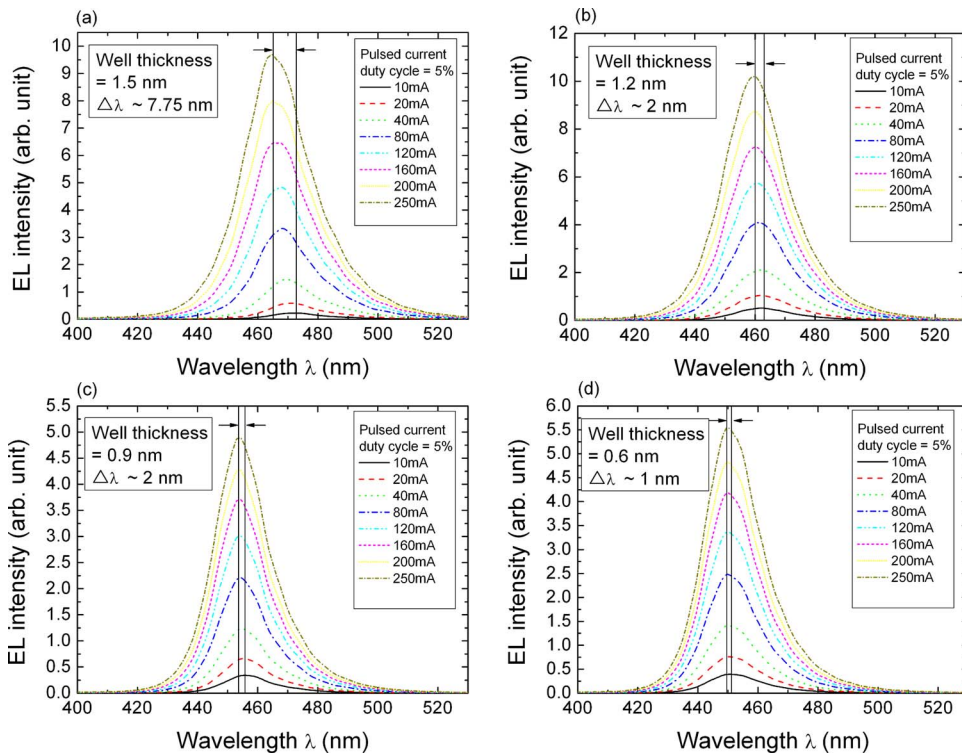


FIG. 3. (Color online) Room-temperature EL spectra of MQW LEDs with varied well thicknesses under various injection currents. The peaks of the emission spectra shift toward shorter wavelengths (blueshift) as the current is increased from 10 to 250 mA, as indicated by the two vertical lines.

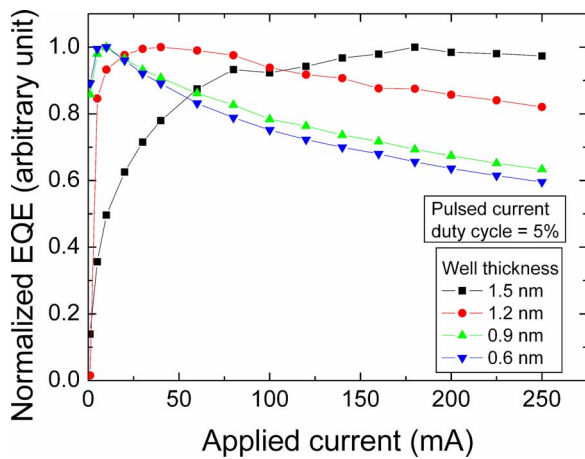


FIG. 4. (Color online) Normalized external quantum efficiency measurements of the MQW LEDs with varied well thicknesses. Measurements are pulsed with 5% duty cycle. For samples with different well thicknesses, the efficiency drop from the highest value at low current density to 200 A/cm² is 2.7%, 17.9%, 36.7%, and 40.4%, respectively. This figure clearly illustrates a reduced efficiency-droop effect for thicker quantum wells.

tion of internal polarization field. A thinner quantum well structure results in less QCSE-induced wavelength shift so that the magnitude of blueshift is less.¹⁰ At the same time, the radiative recombination rate is raised because the reduction of the internal field enhances the spatial overlap of electrons and holes that are otherwise separated by the strong internal field within the MQWs.

Figure 4 shows the normalized external quantum efficiency curves with varied thicknesses of wells under different current densities. To prevent heating, LEDs are operated under pulsed current injection. Investigating Fig. 4 reveals that MQW structures with thick wells could drastically reduce the efficiency droop effect. For samples with well widths of 1.2, 0.9, and 0.6 nm, efficiency peaks can be observed at 25, 7, and 7 mA, respectively. Very little efficiency droop is observed for the LED with the thickest (1.5 nm) well design. In this case, the efficiency drop from the highest value at low current density to 200 A/cm² is less than 3%. We propose that the strong droop effect for InGaN/GaN MQW LEDs is mainly due to the carrier overflow under high applied current densities, consistent with Refs. 11 and 12, instead of thermal heating. LEDs with thicker wells lead to less carrier overflow and thus reduce droop effect. However, since the internal polarization field is too strong to be compensated even under 200 A/cm²,¹³ the thicker well structure results to a larger spatial separation of electrons and holes

and thus reduces the radiative recombination rate, as shown in Fig. 2.

According to the previous discussion, there seems to be a trade-off to achieve both high efficiency and “no droop” for InGaN/GaN LEDs grown along *c*-plane direction. Heavily doping the barriers with Si may help resolve the issue but at the same time, could reduce the material quality and thus enhance nonradiative recombination. The other possibility is to reduce the internal polarization field by material growth along nonpolar direction.

In conclusion, InGaN/GaN-based MQW LEDs with various well thicknesses have been fabricated and characterized. We have demonstrated that the droop effect can be drastically reduced to less than 5% at a current density as high as 200 A/cm². Relative IQE measurements show that thicker well structures lead to a lower radiative recombination rate caused by the larger spatial separation of electrons and holes, which in turn is caused by the strong internal polarization field.

Support by Taiwan National Science Council and Formosa Epitaxy, Inc. is gratefully acknowledged. The authors would like to thank Professor E. F. Schubert and Dr. R. F. Karlicek for fruitful discussions.

- ¹S. Nakamura, M. Senoh, N. Iwasa, and S. Nagahama, *Jpn. J. Appl. Phys.*, Part 2 **34**, L797 (1995).
- ²T. Mukai, S. Nagahama, M. Sano, T. Yanamoto, D. Morita, T. Mitani, Y. Narukawa, S. Yamamoto, I. Niki, M. Yamada, S. Sonobe, S. Shioji, K. Deguchi, T. Naitou, H. Tamaki, Y. Murazaki, and M. Kameshima, *Phys. Status Solidi A* **200**, 52 (2003).
- ³J. K. Kim, T. Gessmann, E. F. Schubert, J.-Q. Xi, H. Luo, J. Cho, C. Sone, and Y. Park, *Appl. Phys. Lett.* **88**, 013501 (2006).
- ⁴Y.-L. Li, E. F. Schubert, and J. W. Graff, *Appl. Phys. Lett.* **76**, 2728 (2000).
- ⁵T. Mukai, M. Yamada, and S. Nakamura, *Jpn. J. Appl. Phys.*, Part 1 **38**, 3976 (1999).
- ⁶M. R. Krames, O. B. Shchekin, R. Mueller-Mach, G. O. Mueller, L. Zhou, G. Harbers, and M. G. Craford, *J. Disp. Technol.* **3**, 160 (2007).
- ⁷Y. C. Lin, S. J. Chang, Y. K. Su, T. Y. Tsai, C. S. Chang, S. C. Shei, C. W. Kuo, and S. C. Chen, *Solid-State Electron.* **47**, 849 (2003).
- ⁸J. Bai, T. Wang, and S. Sakai, *J. Appl. Phys.* **88**, 4729 (2000).
- ⁹T. Wang, D. Nakagawa, M. Lachab, T. Sugahara, and S. Sakai, *Appl. Phys. Lett.* **74**, 3128 (1999).
- ¹⁰A. Hangleiter, J. S. Im, H. Kollmer, S. Heppel, J. Off, and F. Scholz, *MRS Internet J. Nitride Semicond. Res.* **3**, 15 (1998).
- ¹¹M. C. Schmidt, K.-C. Kim, H. Sato, N. Fellows, H. Masui, S. Nakamura, S. P. Denbaars, and J. S. Speck, *Jpn. J. Appl. Phys.*, Part 2 **46**, L126 (2007).
- ¹²K.-C. Kim, M. C. Schmidt, H. Sato, F. Wu, N. Fellows, M. Saito, K. Fujito, J. S. Speck, S. Nakamura, and S. P. Denbaars, *Phys. Status Solidi (RRL): Rapid Res. Lett.* **1**, 125 (2007).
- ¹³G. Franssen, T. Suski, P. Perlin, R. Bohdan, A. Bercha, W. Trzeciakowski, I. Makarowa, P. Prystawko, M. Leszczyński, I. Grzegory, S. Porowski, and S. Kokenyesi, *Appl. Phys. Lett.* **87**, 041109 (2005).